ISSN 2712-8008
Volume / Том 22 №4 2022
Journal Homepage: http://vestnik.pstu.ru/geo/

Perm Journal of Petroleum and Mining Engineering

UDC 622.452
Article / Статья

Study of the influence of aerodynamic processes in a mine shaft with cable reinforcement on vibrations of a moving skip

Mikhail A. Semin, Stanislav V. Maltsev, Evgeny V. Kolesov

Mining Institute of Ural Branch of the Russian Academy of Sciences (78a Sibirskaya st., Perm, 614007, Russian Federation)

Исследование влияния аэродинамических процессов в шахтном стволе с канатной армировкой на колебания движущегося скипа

М.А. Семин, С.В. Мальцев, Е.В. Колесов

Горный институт Уральского отделения Российской академии наук (Россия, 614007, г. Пермь, ул. Сибирская, 78а)

Received / Получена: 22.04.2022. Accepted / Принята: 18.11.2022. Published / Опубликована: 22.12.2022

Keywords:
mine, mine ventilation, skip shaft, air consumption, non-stationary air distribution, turbulent air flow, skip vibrations, rope reinforcement, flow around bodies, aerodynamic force, dynamic meshes, numerical modeling, computational fluid dynamics, finite volume method, boundary layer.

A study of non-stationary air distribution that occurs in a skip shaft with rope reinforcement when two lifting vessels move along it was made. The theoretical analysis of air distribution was carried out using numerical simulation of an unsteady turbulent air flow in the shaft section using the Ansys Fluent software package. To describe the movement of skips, the dynamic grid approach was used, based on the deformation and rebuilding of internal grid cells during the calculation process. Based on the calculated non-stationary distribution of aerodynamic parameters near the moving skips, the total aerodynamic forces acting on the skips were calculated. They were used further to analyze the horizontal vibrations of the skips, taking into account the restrictions imposed by the lifting, balancing and guide ropes. Within the framework of the accepted model simplifications, it was obtained that the maximum values of the aerodynamic forces acting on the skips were observed for the time interval corresponding to the passage of two skips next to each other, in this case the section of the mine shaft overlapped to the maximum. A short-term increase in the aerodynamic force acting on the skip during this period of time led to the appearance of skip oscillations in the horizontal plane. It was shown that the maximum peak value of the horizontal aerodynamic force component significantly depended on the allowance for the movement of skips. This indicated that the analysis of skip oscillations in the wellbore under the assumption of instantaneously resting skips was incorrect. Further, based on the calculated aerodynamic loads on the skips in the course of a series of numerical experiments, the maximum horizontal displacements of each of the skips were determined as a function of the air velocity in the shaft. On the basis of the displacements obtained, approximating dependences for the maximum displacements of the skip were constructed depending on its mass and the average air velocity in the shaft.

Ключевые слова:
рудник, рудничная вентиляция, скиповой ствол, расход воздуха, нестационарное воздухораспределение, турбулентное течение воздуха, колебания скипов, канатная армировка, обтекание тел потоком, аэродинамическая сила, динамические сетки, численное моделирование, вычислительная гидроаэродинамика, метод конечных объемов, пограничный слой.

Проведено исследование нестационарного воздухораспределения, возникающего в скиповом стволе с канатной армировкой при движении по нему двух подъемных сосудов. Теоретический анализ воздухораспределения проводился с помощью численного моделирования нестационарного турбулентного течения воздушного потока на участке ствола в программном комплексе Ansys Fluent. Для описания движения скипов использовался подход динамических сеток, основанный на деформировании и перестроении внутренних ячеек сетки в процессе расчета. Исходя из рассчитанного нестационарного распределения аэродинамических параметров, около движущихся скипов вычислялись суммарные аэродинамические силы, действующие на скипы. Они использовались далее для анализа горизонтальных колебаний скипов с учетом ограничений, накладываемых подъемными, уравновешивающими и направляющими канатами. В рамках принятых модельных упрощений получено, что максимальные значения аэродинамических сил, действующих на скипы, наблюдаются для промежутка времени, соответствующего прохождению двух скипов друг около друга, – в этом случае максимально перекрывается сечение шахтного ствола. Кратковременное возрастание аэродинамической силы, действующей на скип в этот промежуток времени, приводит к появлению колебаний скипа в горизонтальной плоскости. Показано, что максимальная величина пика горизонтальной компоненты аэродинамической силы существенно зависит от учета движения скипов. Это указывает, что анализ колебаний скипов в стволе в предположении о мгновенно покоящихся скипах является некорректным. Далее, исходя из рассчитанных аэродинамических нагрузок на скипы в ходе серии численных экспериментов, определены максимальные горизонтальные смещения каждого из скипов как функции скорости воздуха в стволе. На основании полученных смещений построены аппроксимирующие зависимости для максимальных смещений скипа в зависимости от его массы и средней скорости воздуха в стволе.

© **Mikhail A. Semin** (Author ID in Scopus: 56462570900) – PhD in Engineering, Researcher (tel.: +007 (909) 106 20 67, e-mail: seminma@inbox.ru). The contact person for correspondance.
© **Stanislav V. Maltsev** (Author ID in Scopus: 57215839650) – PhD in Engineering, Head of the Sector (tel.: +007 (909) 106 20 67, e-mail: stasmalcev32@gmail.com).
© **Evgeny V. Kolesov** (Author ID in Scopus: 57213155757) – Junior Researcher (tel.: +007 (909) 106 20 67, e-mail: kolesovev@gmail.com).

© **Семин Михаил Александрович** – кандидат технических наук, научный сотрудник (тел.: +007 (909) 106 20 67, e-mail: seminma@inbox.ru). Контактное лицо для переписки.
© **Мальцев Станислав Владимирович** – кандидат технических наук, заведующий сектором (тел.: +007 (909) 106 20 67, e-mail: stasmalcev32@gmail.com).
© **Колесов Евгений Викторович** – младший научный сотрудник (тел.: +007 (909) 106 20 67, e-mail: kolesovev@gmail.com).

Please cite this article in English as:
Semin M.A., Maltsev C.V., Kolesov E.V. Study of the influence of aerodynamic processes in a mine shaft with cable reinforcement on vibrations of a moving skip. *Perm Journal of Petroleum and Mining Engineering*, 2022, vol.22, no.4, pp.192-200. DOI: 10.15593/2712-8008/2022.4.7

Просьба ссылаться на эту статью в русскоязычных источниках следующим образом:
Семин М.А., Мальцев С.В., Колесов Е.В. Исследование влияния аэродинамических процессов в шахтном стволе с канатной армировкой на колебания движущегося скипа // Недропользование. – 2022. – Т.22, №4. – С.192–200. DOI: 10.15593/2712-8008/2022.4.7

Introduction

The current trend to increase the volume of underground mining, as well as the increasing branching of mining systems in underground horizons leads to the need to supply more air to shafts and mines [1–3]. One of the options for increasing the amount of air supplied to the mine is the use of skip shafts, which are most often neutral in terms of ventilation [4]. As the depth of mining operations increases, the required skip lifting height also increases, and the operation of hoisting ropes becomes more complicated due to torsion, longitudinal and transverse vibrations [5, 6].

The regulatory documents in force in Russia [7] states that in shafts intended only for lowering and lifting of loads, the maximum speed should not exceed 15 m/s. Physically, this is associated with fact that the following problems may occur at high airflow rates in shafts with lifting vessels [8–10]:

1. Vibration of lifting vessels resulting in breakage and destruction.
2. Vibrations in ropes.
3. Possible collision of lifting vessels with rope guides in the middle of the shaft.
4. Knocking against the cross timbers in the area where vehicles pass through.

At the same time, in earlier regulatory documents, the maximum speed of lifting vessels was determined differently. For example, [11] presents the following formula for the maximum speed of lifting vessels when lifting and lowering loads along vertical shafts:

$$V = 0.8\sqrt{H}, \quad (1)$$

where H – shaft height, m.

In monograph [12] the main factors influencing the skip movement are the skip rotation around the vertical axis and translational movements in the horizontal plane. It has been made the assumption that the translational movement of skips in the lateral plane are caused mainly by the Coriolis force [13] and aerodynamic forces as a result of interaction of the skip with the air flow.

Works [14, 15] describe the results of a large series of measurements - in more than ten mines equipped with cable guides. It was found that the Coriolis force is not the main source of skip vibrations, and the calculation methods proposed in [12] are imperfect.

The paper [5] proposes a methodology for determining the parameters of multi-rope hoisting based on the study of dynamic phenomena in hoisting ropes. The conditions of deep mines (up to 2000-2200 m depth) are considered. The efficiency of multi-rope hoisting installations with reduced distance between ropes is investigated.

In works [16, 17] the separate question of of lifting vessels vibration after passing near each other is considered. As a result of coupled modelling of air flow in the shaft and skip motion, it was obtained that with increasing air flow rate in the shaft, the maximum horizontal displacement increases according to a nonlinear law. At the same time, the works do not take into account the resistance from the guides and Coriolis force.

In [18], a theoretical and experimental analysis of the lateral vibration acceleration of a steel skip rope at different air rates was carried out. It was obtained that the acceleration of transverse displacement and longitudinal vibration significantly increases with increasing speed, and due to the presence of transverse vibration there are more extremes of longitudinal vibration acceleration affecting the service life of the rope.

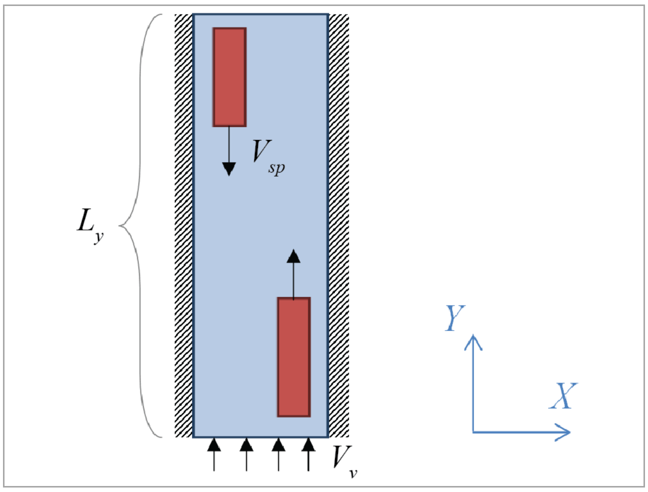

Fig. 1. Geometric model

In [19, 20] the problems of vibrating resonance of lowering skip and ropes without regard to aerodynamic effects from the flow side are investigated. It is noted that in practice a large amplitude of vibrations in the system "skip – ropes" can often occur, steady vibrations can be formed, and can lead to emergency scenarios.

In [4] the aerodynamic loads on the skip during the passage of the channel of the main fan unit and during the passage of two skips near each other were determined by numerical modelling. It was concluded that even at sufficiently high air rate of 18 m/s (exceeding the permissible values) the aerodynamic effect of the air flow on the skip and rope is negligible. However, the dynamic characteristics of skips are not fully considered in this work.

The purpose of the present work, continuing the previous studies [4, 21], is to analyse the force effects of the air flow on the skip with reference to the dynamic characteristics of the skip itself and the aerodynamic properties of the air flow.

Methodology

Determination of force effects from the air flow on the skip in this paper is carried out by numerical modelling in the ANSYS fluent software package. The geometrical model is a section of a mine shaft of length Ly (Fig. 1). The shaft has a diameter D and is a ventilation and skip, and therefore the air flow moves in the direction from bottom to top. The air flow is carried out in the mode of developed turbulence with an average velocity equal to Vv. At this section of the shaft there are also two skips moving in opposite directions with the same speed Vsp. The absolute coordinate system OXY is associated with the barrel, with the X axis pointed horizontally, and the Y axis is vertical. A flat two-dimensional problem is considered, and the selected design domain physically corresponds to the mid-section of the shaft. The skips have given geometrical dimensions – width (in the X direction) and height (in the Y direction).

Isothermal unsteady air flow is described by the continuity and Navier-Stokes equations [22, 23]:

$$\frac{\partial \rho}{\partial t} + \nabla \cdot (\rho V) = 0, \quad (2)$$

$$\frac{\partial}{\partial t}(\rho V) + \nabla \cdot (\rho V V) = -\nabla p + \nabla \cdot \tau + \rho g, \quad (3)$$

where V – vector of air flow rate, m/s; p – pressure, Pa; g – vector of free-fall acceleration, m/s^2; – shear stress tensor [24], Pa:

$$T = (\mu + \mu_t)\left[\nabla V + (\nabla V)^T\right], \quad (4)$$

where μ – molecular viscosity of air, P·s; μ_t – turbulent viscosity, Pa-s.

In the framework of the SST k-omega turbulence model used here [25, 26], the turbulent viscosity is represented as:

$$\mu_t = \rho \frac{a_1 k}{\max\left(a_1\omega, 2\sqrt{\mathbf{S}\cdot\cdot\mathbf{S}}F_2\right)}, \quad (5)$$

where k – specific turbulent kinetic energy, m²/s²; ω – the specific energy of turbulent dissipation, 1/s; a_1 – *SST* model parameter; *F2* - second smoothing function [27]; *S* – strain rate tensor, 1/s.

Turbulent airflow characteristics k and ω are determined by solving the two transfer equations:

$$\frac{\partial}{\partial t}(\rho k) + \nabla\cdot(\rho k \mathrm{V}) = \nabla\cdot(\Gamma_k \nabla k) + \tau\cdot\cdot\nabla\mathrm{V} - \beta^*\rho\omega k, \quad (6)$$

$$\frac{\partial}{\partial t}(\rho\omega) + \nabla\cdot(\rho\omega\mathrm{V}) = \nabla\cdot(\Gamma_\omega \nabla k) + 2\alpha\mathrm{S}\cdot\cdot\mathrm{S} - \beta\rho\omega^2 - 2(1-F_1)\sigma_{\omega 2}\frac{\rho}{\omega}\nabla k\cdot\nabla\omega, \quad (7)$$

where Γ_k и Γ_ω – effective diffusion coefficients for turbulent characteristics of the medium k and ω; F_1 – the first smoothing function; α, β, β^* and $\sigma_{\omega 2}$ – model parameters [25, 27].

At the entrance to the computational area (lower boundary), a uniform field of air flow rates, a given turbulence intensity, and the ratio of effective viscosity to molecular viscosity are set. At the outlet of the computational area, the static pressure is set. On solid walls, the condition of flow adhesion is set. The distribution of temperatures is uniform everywhere.

The numerical solution of equations (2)-(7) with appropriate initial and boundary conditions is carried out by the finite volume method using the Semi-Implicit Method for Pressure-Linked Equations (SIMPLE) algorithm [28, 29]. The second order of spatial discretisation and the first order of temporal discretisation are used for all the sought variables. To accelerate the numerical calculation, parallelisation is performed on four CPU cores.

Modelling of skip motion is carried out within the framework of dynamic meshes approach [30, 31]. To smooth the deforming mesh, the Spring-based smoothing method [32] is used, which is based on the representation of mesh faces between any two nodes as interconnected springs of a given reinforcement. The Laplace smoothing method is also used, which adjusts the location of each mesh vertex at the geometric centre of neighbouring vertices [33].

At each time step of the numerical calculation algorithm, local rearrangement of the mesh near the moving skips is performed by the Local cell method [34, 35]. In this case, the programme agglomerates cells based on asymmetry, size and height criteria (adjacent zones of moving faces) before moving the boundary. The size criteria are specified using a given minimum length scale h_{min} and maximum length scale h_{max}. A maximum mesh asymmetry value is also set, indicating the desired mesh asymmetry.

The cells corresponding to the boundary layers of each of the skips and the shaft walls are not deformed or rearranged during the numerical calculation. In this case, the set of boundary layer cells of each skip moves together with the corresponding skip as a single non-deformable solid body.

The flow calculation is performed in a two-dimensional formulation for the above described two-dimensional geometrical domain. Methodologically, this idealisation is related to the desire to conduct and debug a complex and resource-intensive numerical algorithm with dynamic meshes on a relatively simple two-dimensional model. In further research, the authors also plan to consider the three-dimensional case.

As a result of interaction of the moving skips with the air flow, non-uniform load is formed on the non-deformable walls of the skips, which changes with time. To analyse skip movements under the action of aerodynamic load from the air stream, the total vector forces F_1 and F_2 acting on the skips are calculated. When calculating these forces, the third spatial dimension of the skips, previously not explicitly taken into account at modelling two-dimensional air flow in the shaft, is considered. They are used to determine lateral movements of the skips, satisfying the following equation [16]:

$$m_i \frac{\partial^2 X_i}{\partial t^2} = -k_i X_i + F_i^{(X)} \pm F_i^{(cor)}, \quad (8)$$

$$m_i \frac{\partial^2 Y_i}{\partial t^2} = -k_i Y_i + F_i^{(Y)}, \quad (9)$$

where m_i – mass of i skip, kg; X_i and Y_i – displacements of the i-$_{th}$ skip in the direction of X and Y axes, respectively, m; $F_i^{(cor)}$ – Coriolis force, N; k – transverse equivalent "spring" stiffness resulting from interaction of the skip with hoisting and balancing ropes, guide ropes.

The equivalent spring reinforcement of the ropes in relation to the horizontal displacements of the skip can be found by the formula [17, 36]:

$$k = n_R \frac{T_L L}{L_1 L_2} + n_H \frac{T_H}{L_1} + n_T \frac{T_T}{L_2}, \quad (10)$$

where n_R – number of guiding ropes per skip; T_L – tension of guide ropes at the skip height in the shaft, N; L – total length of guide ropes, m; L_1 – distance between the shaft mouth and the hoisting rope suspension gear, L_2 – distance between the balance rope suspension gear and the sump, m; n_H – number of hoisting ropes per skip, T_H – tension of the hoisting rope during transportation, N; n_T – number of balancing ropes for one skip; T_T – tension of the balancing rope during transportation, Pa.

In the most pessimistic scenario, it is assumed that the tension of the guide and balance ropes is only due to their own weight. In this situation, the main contribution to the expression (10) will be made by the summand No. 2 on the right. And when substituting it into equation (8), the latter in mathematical form and physical meaning will be very close to the equation of a mathematical pendulum of variable length [37, 38]. In this case, it is important to additionally take into account in equation (8) the summand characterising the Coriolis force. In equation (8) it is written with variable sign, as far as, depending on the direction of skip movement along the shaft it can have both positive effect (damping horizontal oscillations) and negative one. The hoist rope tension is determined only by the weight of the skip, and the effects of skip acceleration/deceleration are not taken into consideration (for the centre part of the shaft this assumption is quite reasonable).

The approach used here does not bear in view vibrations in the ropes themselves, which may arise as a result of interaction with the vibrating skip and with the air flow.

Numerical calculation of time dependencies *Xi(t)* and *Yi(t)* is carried out using the finite difference method, an explicit scheme of the second order of accuracy with respect to the time step [39, 40]. According to these dependences it is possible to determine the maximum values of horizontal displacements of skips during their movement along the skip. It is assumed that the most unfavourable moment leading to destabilization of the skips position in space is when skips pass each other.

In addition, this approach assumes that the skip does not rotate around its centre of mass and has only two degrees of freedom, *Xi* and *Yi*. Consideration of the rotational degree of freedom is supposed to be realised in further studies of the authors.

Results and discussion

The parameters of the problem used for numerical calculations are summarised in Table 1.

A series of numerical experiments were carried out at different mesh parameters, aerodynamic parameters of the problem. The duration of one calculation was from 5 to 12 h. (depending on the selected parameters). The calculations were performed on a personal computer equipped with a 6-core Intel Core i7-8700K CPU (3.70GHz) and 16 GB of RAM. The results of numerical simulation were visualised in the ANSYS CFD-Post software module and in Wolfram Mathematica.

Figure 2 shows the calculated distribution of air rate magnitudes at different time moments with an average air rate in the shaft equal to 2.5 m/s.

In this situation, skips move faster than the air flow. As can be seen from Fig. 2, behind skip No 1, going down the shaft, an unstable non-stationary structure of air flows is formed caused by the periodic breakdowns of the air flow from the sharp edges of this skip. At the same time, a similar effect is not observed for the upward skip No 2. This conclusion is valid in a wide range of studied mesh parameters and time steps (see Table 1). This can be verified by plotting the time dependences of the horizontal (*X*) component of the aerodynamic force acting on the skips at different time steps (Fig. 3) and different space steps (Fig. 4). The aerodynamic force components were plotted by Ansys CFD-Post basic commands [41, 42] – they take into account both the total airflow pressure acting along the normal to the skip wall and the shear friction resistance due to air viscosity and acting tangential to the wall.

Figs. 3, 4 also show the characteristic peak of aerodynamic load at the moment of time about 12 s. This peak is caused by the passage of two skips relative to each other. The time dependences of aerodynamic forces for both skips in the vicinity of the peak are described approximately the same for the considered set of spatial and temporal steps. At the same time, this peak is the main source of horizontal vibrations of the skips [16] as they move along the shaft, while relatively small deviation of aerodynamic forces over the remaining time interval have little effect on these vibrations. A similar vibratory character of the time dependences for the aerodynamic forces was also obtained in [16, 17].

The peak magnitude depends significantly on the average air flow rate in the shaft (Fig. 5).

The increase in peak amplitude with increasing air flow rate is evident for both skips. The amplitude of flow disruption vibrations also increases, which is especially noticeable for the descending skip (see Fig. 5, *b*). At high air rates (12.5 m/s) flow stalls also start to occur for the upward skip, whose movement is co-directed with the air flow. This indicates that the phenomenon of flow breakdown is determined first of all by the speed of the skip relative to the air flow.

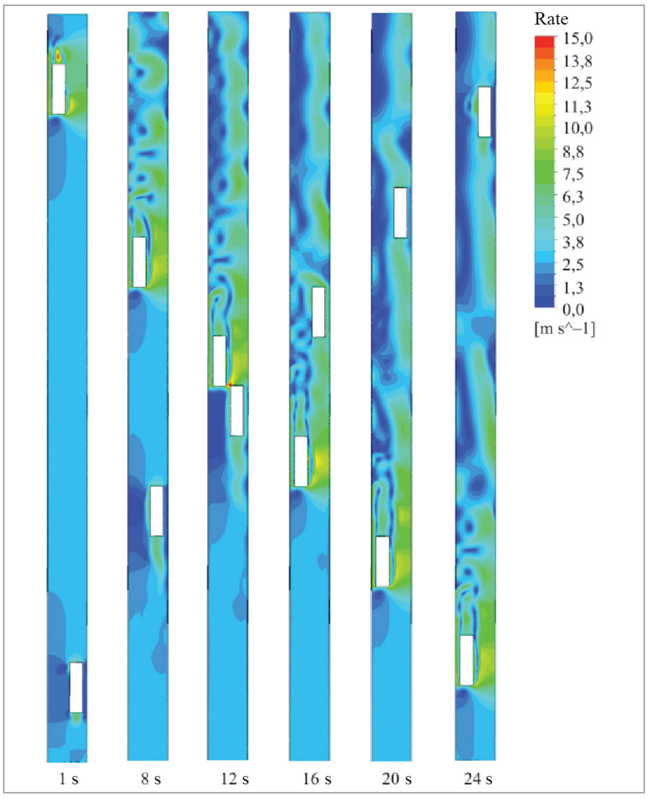

Fig. 2. Magnitude distribution of the rate of air flow around moving skips

Table 1

Numerical parameters of the problem

Parameter	Value
Shaft diameter, m	8
Length of the shaft section under consideration, m	150
Shaft length, m	1000
Skip width (along *X*), m	2.5
Skip width (along *Z*), m	2.3
Skip height (*Y*), m	10
Weight of unloaded skip, tonnes	19
Weight of loaded skip, tonnes	49
Number of hoisting ropes per skip	2
Number of balancing ropes for one skip	4
Number of guiding ropes per skip	4
Horizontal equivalent spring stiffness of ropes of unloaded skip, kN/m	2.01
Horizontal equivalent spring stiffness of the loaded skip ropes, kN/m	5.16
Speed of skip movement, m/s	5
Air rate at the inlet, m/s	2.5–15
Turbulence intensity at the inlet	5 %
Ratio of effective viscosity to inlet molecular viscosity	10
Modelling time, s	24
Time step, s	0.0025–0.02
Maximum number of sub-steps in time	70
Minimum permissible relative error of connection	10^{-4}
Mesh cell size, m	0.12–0.3
Minimum length scales h_{min}, m	0.15
Maximum length scales h_{max}, m	0.3
Target mesh asymmetry	0.6
Number of boundary layers	5
Y+ (defined after preliminary modelling)	42–210

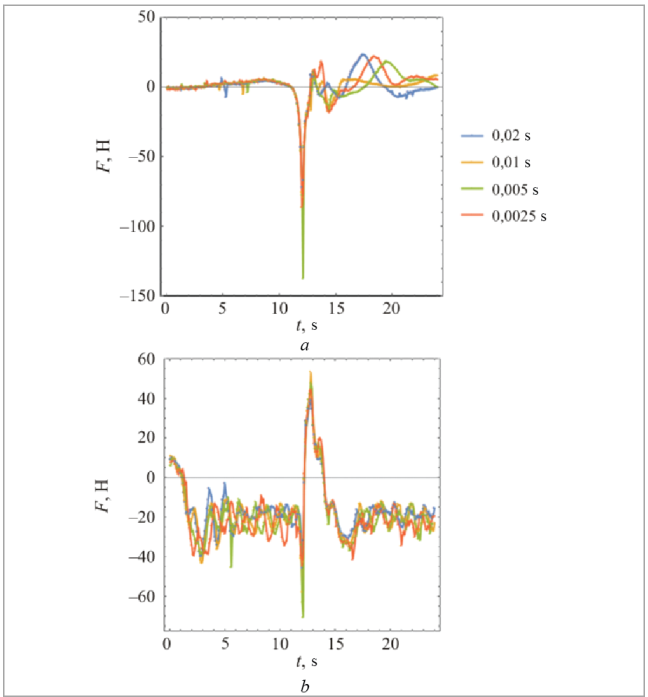

Fig. 3. Time dependences of the horizontal component of the aerodynamic force acting on the rising (*a*) and lowering (*b*) skips at different time steps

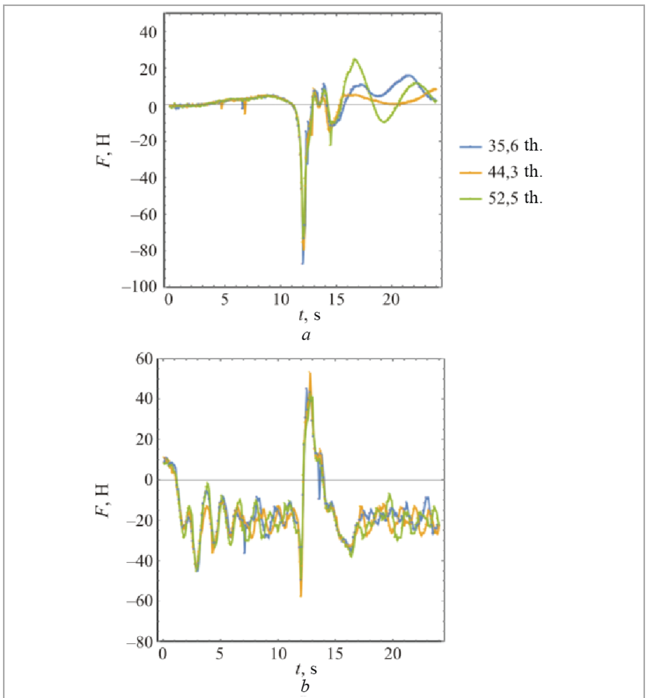

Fig. 4. Time dependences of the horizontal component of the aerodynamic force acting on the rising (*a*) and lowering (*b*) skips at different number of cells of calculation meshes

The maximum value of the peak of the horizontal component of the aerodynamic force depends significantly on the skip motion. If the problem is solved with the assumption of instantaneous rest of each skip at each moment of time, the resulting aerodynamic loads will be different (Table 2, fixed mesh). In this case, the discrepancies between the different solutions (with and without consideration of the skip dynamics) are very large (sometimes the solutions differ by a factor of 10). This is associated with the fact that at the instantaneous rest of each of the skips at each moment of time, the piston effect

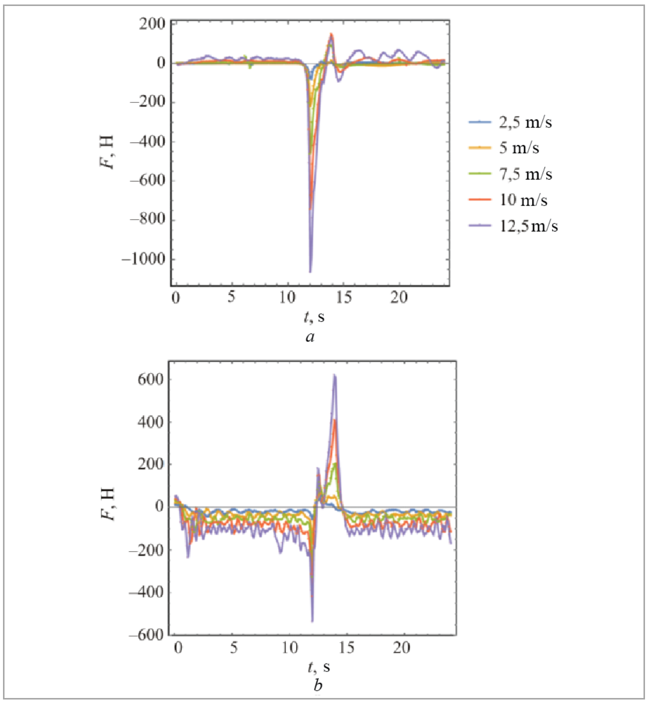

Fig. 5. Time dependences of the horizontal component of the aerodynamic force acting on the rising (*a*) and lowering (*b*) skips at different rate of air flow

created by the skips during movement is not taken into account and significantly determines the rate of the air flow between the skips at the moment when they are at the same altitude mark.

Fig. 6 shows the total pressure distributions near two skips at the moment they pass near each other. The total pressure in this situation is a relative value (since zero static pressure is recorded at the outlet of the design area), and therefore negative values of total pressure are observed in local zones. The fields correspond to the average rate of the air flow in the shaft equal to 15 m/s. 6, a, corresponds to the consideration of the real speed of the skip and dynamic reconstruction of the mesh. The case in Fig. 6, *b*, corresponds to the assumption of the instantaneous rest of each of the skips. Pressure distributions near the sidewalls of skips vary significantly in these two situations. In the case of a fixed mesh (see Fig. 6, *b*) in the upper part of the skips there are low pressure zones (blue), which are asymmetrically distributed on the sides of the skip and make a significant contribution to the calculation of the total force acting on the skip on the airflow side.

If we analyse the variation of the vertical component of the aerodynamic force acting on the skip during its movement, for both skips it varies in the range from 0 to 350 N (in the range of air flow rate from 2.5 to 15 m/s). This is a quite small value compared to the unloaded weight of the skip (19 tonnes). This indicates that much more significant vertical (longitudinal) vibrations will be formed during acceleration and braking of the skip, while the aerodynamic factor in this case is negligible. For this reason, equation (9) will not be analysed here.

The situation is different for the horizontal vibrations of skips, where the aerodynamic effect of the air flow can be significant. To analyse the horizontal vibrations of each of the skips, a numerical solution of the differential equation (8) was obtained providing for the time dependencies calculated above in Fig. 5. 5. The time step was taken equal to 0.1 s.

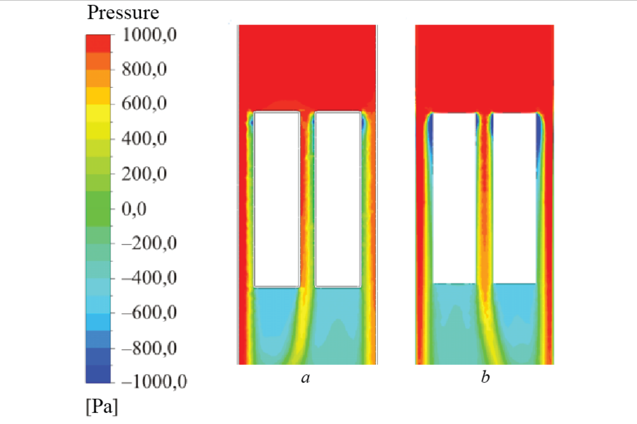

Fig. 6. Distribution of total pressure near skips for dynamic meshes (*a*) and fixed meshes (*b*)

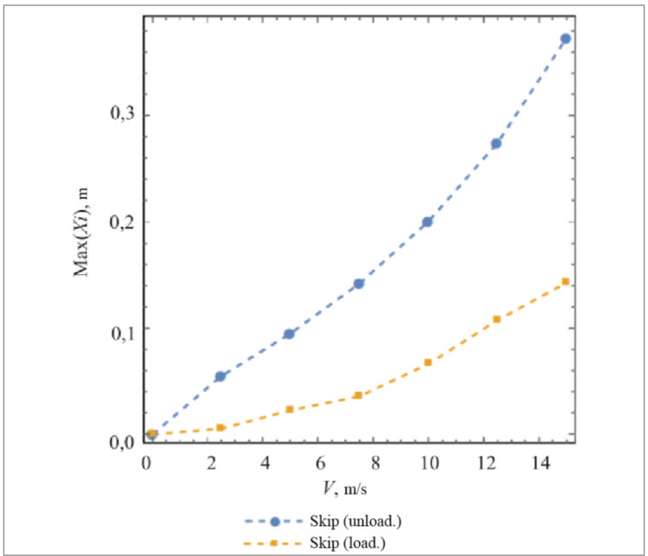

Fig. 7. Dependences of the maximum amplitudes of horizontal vibrations of skips on the air flow rate

Table 2

Comparative Analysis of Horizontal Components of Aerodynamic Force at Different Problem Formulations

Peculiarities of the problem formulation	Skip	Air rate, m/s		
		5	10	15
Dynamic meshes	№ 1	204.6	411.3	936.9
	№ 2	92.8	153.3	211.0
Fixed mesh	№ 1	174.0	696.48	1535.4
	№ 2	323.8	1300.5	2968.2

Fig. 7 shows the calculated dependences of the maximum amplitudes of horizontal skip vibrations on the air flow rate. The dots indicate the results of individual numerical experiments, and the dashed lines indicate piecewise linear interpolation of the solution between the points. As can be seen from the figure, the growth of the vibration magnitude follows a nonlinear law with acceleration. This agrees well with the works [1, 17].

In the considered case, the amplitudes of vibrations in absolute magnitude reach 40 cm for an unloaded skip going downwards and 13 cm for a loaded skip going upwards. These are rather high values, but it should be taken into account that the obtained vibration amplitudes strongly depend on the equivalent reinforcement of the ropes in relation to the horizontal movements of the skip, while the latter were chosen based on the most pessimistic estimation. When the equivalent rope reinforcement is increased by 2 times (e.g. by tensioning the guide ropes) the amplitude of vibrations for the unloaded skip decreases to 21 cm (by 47 %), and for the loaded skip - to 10 cm (by 10 %).

Further, using the least squares method [43, 44] approximating nonlinear degree dependences for the calculated points from Fig. 7 were obtained:

$$X_1 = \frac{0.018V_в^2}{m_1}, \tag{11}$$

$$X_2 = \frac{0.022V_в^2}{m_2}, \tag{12}$$

where X_1 – maximum horizontal displacement of unloaded skip No.1, m; X_2 – maximum horizontal displacement of unloaded skip No.2, m; m_1 – the mass of unloaded skip No. 1, tonnes; m_2 – the mass of loaded skip No. 2, tonnes $V_в$ – average cross-sectional rate of air flow, m/s.

Dependences (11)-(12) were obtained for the case of skip speed of 5 m/s. It is assumed that this parameter should also strongly influence the value of horizontal displacements of skips, however, this issue is not investigated in the present work, but is the subject of further research. In future it is planned to investigate the influence of skip speed and geometrical characteristics of the skip on the peculiarities of its horizontal vibrations, as well as to evaluate the influence of interfaces with horizons and main fan channel on horizontal vibrations. The issues of stability of air distribution in shafts with moving skips are also of practical interest [45, 46], as well as the regularities of transfer of harmful impurities (dust) emitted from the skip surfaces [47–49].

Conclusion

Within the framework of the research described in the article the algorithm for calculation of aerodynamic loads on skips moving along the ventilation-skip shaft is proposed. The algorithm is based on the numerical solution of the continuity, Navier-Stokes and transfer equations of turbulent characteristics of the air flow in ANSYS Fluent software, and also implements dynamic rebuilding of the calculation mesh in the process of modelling the movement of skips and air flow.

Data on aerodynamic loads are used to calculate the total aerodynamic forces acting on skips during their movement. It was obtained that the maximum value of the peak of the horizontal component of the aerodynamic force depends significantly on the skip movement. This indicates that the analysis of skip vibrations in the shaft under the assumption of instantaneously resting skips is incorrect.

It was determined that the maximum values of the aerodynamic force occur when two skips pass each other – in this case, the cross-section of the mine shaft is overlapped as much as possible Short-term increase of the aerodynamic force acting on the skip leads to vibration of the skip in the horizontal plane. The maximum amplitude of vibration increases with the increase of air rate in the shaft. For an unloaded skip the maximum amplitude of vibration is higher than for an unloaded skip. The effective reinforcement of the ropes in relation to the horizontal vibrations of the system has a significant effect on the maximum amplitude of skip vibrations, and therefore special attention should be paid to setting this parameter in practical calculations of skip movement in the air space of the shaft.

References

1. Karelin V.N., Kravchenko A.V., Levin L.Iu., Kazakov B.P., Zaitsev A.V. Osobennosti formirovaniia mikroklimaticheskikh uslovii v gornykh vyrabotkakh glubokikh rudnikov [Features of the formation of microclimatic conditions in the mine workings of deep mines]. *Gornyi zhurnal*, 2013, no. 6, pp. 65-68.
2. Kazakov B.P., Trushkova N.A., Zaitsev A.V. Primenenie chastichnogo povtornogo ispol'zovaniia vozdukha dlia snizheniia kolichestva vypadaiushchei vlagi v kaliinykh rudnikakh [Application of partial reuse of air to reduce the amount of moisture precipitate in potash mines]. *Vestnik Permskogo natsional'nogo issledovatel'skogo politekhnicheskogo universiteta. Geologiia, neftegazovoe i gornoe delo*, 2012, no. 3, pp. 129-133.
3. Kazakov B.P., Mal'tsev S.V., Semin M.A. Sposob optimizatsii parametrov raboty neskol'kikh glavnykh ventiliatornykh ustanovok dlia proektirovaniia energoeffektivnykh rezhimov provetrivaniia rudnikov slozhnoi topologii [Working parameters optimization technique for several main ventilation installations to design energy-efficient modes of mines of complex topology aeration]. *Izvestiya vysshih uchebnyh zavedenij. Gornyj zhurnal*, 2017, no. 1, pp. 101-108.
4. Pospelov D.A., Zaitsev A.V., Semin M.A. Obosnovanie maksimal'noi dopustimoi skorosti vozdukha v stvolakh po faktoru aerodinamicheskoi nagruzki na tekhnologicheskoe oborudovanie [Justification of the maximum allowable air speed in the shafts by the factor of aerodynamic load on process equipment]. *Gornoe ekho*, 2020, no. 1, pp. 90-94. DOI: 10.7242/echo.2020.1.19
5. Zhigula T.I. Obosnovanie parametrov shakhtnykh mnogokanatnykh pod"emnykh ustanovok na osnove issledovaniia prodol'no-poperechnykh kolebanii kanatov [Justification of the parameters of mine multi-rope lifting installations based on the study of longitudinal-transverse vibrations of ropes]. Ph. D. thesis, 1985, 202 p.
6. Tauger V.M., Volkov E.B., Leont'ev A.A. Teoretiko-mekhanicheskii raschet ustoichivosti dvizheniia sosuda v shakhtnoi skipovoi pnevmopod"emnoi ustanovke [Theoretical mechanical calculations of the stability of the vessel motion in a mine skip pneuvmo elevating equipment]. *Izvestiia Ural'skogo gosudarstvennogo gornogo universiteta*, 2018, no. 1 (49). pp. 89-93. DOI: 10.21440/2307-2091-2018-1-68-79
7. Pravila bezopasnosti pri vedenii gornykh rabot i pererabotke tverdykh poleznykh iskopaemykh: federal'nye normy i pravila v oblasti promyshlennoi bezopasnosti utv. 08.12.2021, № 505 [Safety rules for mining operations and processing of solid minerals: federal norms and rules in the field of industrial safety approved. 12/08/2021, No. 505]. Moscow, 2021.
8. Brake D.J. Mine Ventilation: A Practitioner's Manual. Brisbane, Australia, 2013, 791 p.
9. McPherson M.J. An analysis of the resistance and airflow characteristics of mine shafts. *Fourth International Mine Ventilation Congress*, 1988. Brisbane, Queensiand, 8 p.
10. Yao J., Deng X., Ma C., Xu T. Investigation of Dynamic Load in Superdeep Mine Hoisting Systems Induced by Drum Winding. *Shock and Vibration*, 2021, vol. 2021, 4756813 p. DOI: 10.1155/2021/4756813
11. Edinye pravila bezopasnosti pri razrabotke rudnykh, nerudnykh i rossypnykh mestorozhdenii podzemnym sposobom [Uniform safety rules for the development of ore, non-ore and alluvial deposits by underground mining]. Moscow: Nedra, 1972, 224 p.
12. Belyi V.D. Kanatnye provodniki shakhtnykh pod"emnykh ustanovok [Rope guides for mine hoists]. Moscow: Ugletekhizdat, 1959, 212 p.
13. Stradanchenko S.G., Prokopov A.Iu., Tkacheva K.E. Veroiatnostnyi podkhod k opredeleniiu vremennykh nagruzok na zhestkuiu armirovku vertikal'nykh stvolov [Probabilistic approach to determination of the tempral loadings on reinforcement of vertical shafts]. *Gornyi informatsionno-analiticheskii biulleten' (nauchno-tekhnicheskii zhurnal)*, 2012, no. 8, pp. 61-68.
14. Chen X. Analysis of the Soviet calculation formula for the clearance between rope-guided conveyance and conveyance. *Design of Coal Mine (China)*, 1979, vol. 26, no. 4, pp. 17-23.
15. Chen X. Swing of hoisting conveyance using steel rope guides. *Coal Science and Technology (China)*, 1985, vol. 13, no. 2, pp. 23-26.
16. Wu R., Zhu Z., Cao G. Computational Fluid Dynamics Modeling of Rope-Guided Conveyances in Two Typical Kinds of Shaft Layouts. *PLoS One*, 2015, vol. 17, no. 2, pp. 978-987. DOI: 10.1371/journal.pone.0118268
17. Wu R., Zhu Z., Chen G., Cao G., Li W. Simulation of the lateral oscillation of rope-guided conveyance based on fluid-structure interaction. *Journal of Vibroengineering*, 2014, vol. 16, no. 3, pp. 1555-1563.
18. Ma C., Yao J., Xiao X., Di X., Jiang Y. Vibration Analysis of Winding Hoisting System based on ADAMS/Cable. *Journal of Physics: Conference Series*. IOP Publishing, 2021, vol. 1750, no. 1, Art. no. 012033. DOI: 10.1088/1742-6596/1750/1/012033
19. Wang N., Cao G., Yan L. The Study of Hoisting System for Vertical Shaft Construction Without the Protection of Guided-cable. *8th Symposium on Lift and Escalator Technologies*, 2018, vol. 8, no. 1, pp. 153-159.
20. Ji-hu B.A.O., Peng Z., Chang-ming Z.H.U. Modeling and control of longitudinal vibration on flexible hoisting systems with time-varying length. *Procedia Engineering*, 2011, vol. 15, pp. 4521-4526. DOI: 10.1016/j.proeng.2011.08.849
21. Pospelov D.A., Zaitsev A.V., Semin M.A., Mal'tsev S.V., Mizonov E.N. Povyshenie energoeffektivnosti sistemy ventiliatsii glubokogo rudnika za schet izmeneniia aerodinamicheskikh parametrov skipovogo stvola [Enhancement of ventilation system energy efficiency through the change of aerodynamic characteristics in skip shafts in deep mines]. *Gornyi informatsionno-analiticheskii biulleten' (nauchno-tekhnicheskii zhurnal)*, 2021, no. 9, pp. 135-144. DOI: 10.25018/0236_1493_2021_9_0_135
22. Semin M., Levin L. Theoretical study of partially return air flows in vertical mine shafts. *Thermal Science and Engineering Progress*, 2021, vol. 23, Art. no. 100884. DOI: 10.1016/j.tsep.2021.100884
23. Levin L.Iu., Isaevich A.G., Semin M.A., Gazizullin R.R. Issledovanie dinamiki pylevozdushnoi smesi pri provetrivanii tupikovoi vyrabotki v protsesse raboty kombainovykh kompleksov [Investigation of the dynamics of the dust-air mixture during the ventilation of a dead-end working in the process of operation of combine complexes]. *Gornyi zhurnal*, 2015, no. 1, pp. 72-75. DOI: 10.17580/gzh.2015.01.13
24. Parente E., Farano M., Robinet J.C., De Palma P., Cherubini S. Continuing invariant solutions towards the turbulent flow. *Philosophical Transactions of the Royal Society A*, 2022, vol. 380, no. 2226, Art. no. 20210031. DOI: 10.1098/rsta.2021.0031
25. Menter F.R. Two-Equation Eddy-Viscosity Turbulence Models for Engineering Applications. *AIAA Journal*, 1994, vol. 32, no. 8, pp. 1598-1605. DOI: 10.2514/3.12149
26. Adanta D., Fattah I.M.R., Muhammad N.M. Comparison of standard k-epsilon and SST k-omega turbulence model for breastshot waterwheel simulation. *Journal of Mechanical Science and Engineering*, 2020, vol. 7, no. 2, pp. 39-44. DOI: 10.36706/jmse.v7i2.44
27. Semin M., Golovatyi I., Pugin A. Analysis of Temperature Anomalies during Thermal Monitoring of Frozen Wall Formation. *Fluids*, 2021, vol. 6, no. 8, Art. no. 297. DOI: 10.3390/fluids6080297
28. Lee J., Hong J.W., Lee K., Hong J., Velasco E., Lim Y.J., Park J. Ceilometer monitoring of boundary-layer height and its application in evaluating the dilution effect on air pollution. *Boundary-Layer Meteorology*, 2019, vol. 172, no. 3, pp. 435-455. DOI: 10.1007/s10546-019-00452-5
29. Jandaghian Z. Flow and pollutant dispersion model in a 2D urban street canyons using computational fluid dynamics. *Computational Engineering and Physical Modeling*, 2018, vol. 1, no. 1, pp. 83-93. DOI: 10.22115/CEPM.2018.122506.1014
30. Dumont K., Stijnen J.M.A., Vierendeels J., Van De Vosse F.N., Verdonck P.R. Validation of a fluid-structure interaction model of a heart valve using the dynamic mesh method in fluent. *Computer methods in biomechanics and biomedical engineering*, 2004, vol. 7, no. 3, pp. 139-146. DOI: 10.1080/10255840410001715222
31. You Y., Wang S., Lv W., Chen Y., Gross U. A CFD model of frost formation based on dynamic meshes technique via secondary development of ANSYS fluent. *International Journal of Heat and Fluid Flow*, 2021, vol. 89, Art. no. 108807. DOI: 10.1016/j.ijheatfluidflow.2021.108807
32. Mrinal K.R., Siddique M.H., Samad A. A transient 3D CFD model of a progressive cavity pump. *Turbo Expo: Power for Land, Sea, and Air*. American Society of Mechanical Engineers, 2016, vol. 49873, Art. no. V009T24A009. DOI: 10.1115/GT2016-56599
33. Hai Y., Cheng S., Guo Y., Li S. Mesh smoothing algorithm based on exterior angles split. *Plos one*, 2020, vol. 15, no. 5, Art. no. e0232854. DOI: 10.1371/journal.pone.0232854
34. Zhou H., Zhong K., Jia H., Kang Y. Analysis of the effects of dynamic mesh update method on simulating indoor airflow induced by moving objects. *Building and Environment*, 2022, Art. no. 108782. DOI: 10.1016/j.buildenv.2022.108782
35. Adedeji O.E., Duarte C.A. R. Prediction of thickness loss in a standard 90° elbow using erosion-coupled dynamic mesh. *Wear*, 2020, vol. 460, 203400 p. DOI: 10.1016/j.wear.2020.203400
36. Krige G.J. Guidelines for the design of rope guides. *International Conference on Hoisting and Haulage 2005*. Perth, Australia, 2005, pp. 275-283.
37. Russkikh S.V., Shkliarchuk F.N. Primenenie metoda Bubnova-Galerkina dlia rascheta nelineinykh kolebanii matematicheskogo maiatnika peremennoi dliny pri konechnom peredvizhenii iz odnogo sostoianiia pokoia v drugoe [Using the Bubnov—Galerkin method to calculate the nonlinear oscillations of the variable-length mathematical pendulum at final movement from one state of rest into another]. *Inzhenernyi zhurnal: nauka i innovatsii*, 2018, no. 10 (82), pp. 1-15. DOI: 10.18698/2308-6033-2018-10-1809
38. Surikov I.Iu., Subbota A.D., Tarkhov D.A. Primenenie novykh metodov resheniia differentsial'nykh uravnenii k zadache stabilizatsii perevernutogo maiatnika [Application of new methods for solving differential equations to the problem of stabilization of an inverted pendulum]. *Neirokomp'iutery i ikh primenenie*, 2018, pp. 358-359.
39. Shtetter Kh. Analiz metodov diskretizatsii dlia obyknovennykh differentsial'nykh uravnenii [Analysis of discretization methods for ordinary differential equations]. Moscow: Mir, 1978, 461 p.
40. Mingalev I.V. et al. Iavnaia skhema rasshchepleniia dlia uravnenii Maksvella [The explicit splitting scheme for Maxwell's equations]. *Matematicheskoe modelirovanie*, 2018, vol. 30, no. 12, pp. 17-38. DOI: 10.1134/S2070048219040094
41. Kulshreshtha A., Gupta S.K., Singhal P. FEM/CFD analysis of wings at different angle of attack. *Materials Today: Proceedings*, 2020, vol. 26, pp. 1638-1643. DOI: 10.1016/j.matpr.2020.02.342
42. Song B., Li Y., Sun J., Qi Y., Li P., Li Y., Gu Z. Computational fluid dynamics simulation of changes in the morphology and airflow dynamics of the upper airways in OSAHS patients after treatment with oral appliances. *PloS one*, 2019, vol. 14, no. 11, Art. e0219642. DOI: 10.1371/journal.pone.0219642

43. Brook R.J., Arnold G.C. Applied regression analysis and experimental design. CRC Press, 2018.
44. Golovanchikov A.B., Doan M.K., Petrukhin A.V., Merentsov N.A. Sravnenie tochnosti approksimatsii eksperimental'nykh dannykh metodom naimen'shikh otnositel'nykh kvadratov s metodom naimen'shikh kvadratov [Comparison of the accuracy of experimental data approximation using the least relative squares method with the least squares method]. *Modelirovanie, optimizaciya i informacionnye tekhnologii*, 2020, vol. 8, no. 1, pp. 38-39. DOI: 10.26102/2310-6018/2020.28.1.042
45. Levin L.Iu., Kormshchikov D.S., Semin M.A. Reshenie zadachi operativnogo rascheta raspredeleniia produktov goreniia v seti gornykh vyrabotok [Rapid determination of combustion gas distribution in mine workings]. *Gornyi informatsionno-analiticheskii biulleten' (nauchno-tekhnicheskii zhurnal)*, 2013, no. 12, pp. 179-184.
46. Kazakov B.P., Levin L.Iu., Shalimov A.V., Zaitsev A.V. Razrabotka energosberegaiushchikh tekhnologii obespecheniia komfortnykh mikroklimaticheskikh uslovii pri vedenii gornykh rabot [Development of energy-saving technologies providing comfortable microclimate conditions for mining]. *Zapiski Gornogo instituta*, 2017, vol. 223, pp. 116-124. DOI: 10.18454/pmi.2017.1.116
47. Feng X., Geng F., Teng H., Gui C., Wu S., Li S., Yuan S. Field measurement and numerical simulation of dust migration in a high-rise building of the mine hoisting system. *Environmental Science and Pollution Research*, 2022, vol. 29, no. 25, pp. 38038-38053. DOI: 10.1007/s11356-022-18605-4
48. Isaevich A.G., Kormshchikov D.S. Issledovanie pylevoi obstanovki v usloviiakh kaliinogo rudnika, opyt snizheniia zapylennosti atmosfery rabochikh mest [Investigation of dust conditions in a potash mine, experience in dust reduction in the working areas]. *Izvestiia Tul'skogo gosudarstvennogo universiteta. Nauki o zemle*, 2018, no. 4, pp. 60-74.
49. Liskova M.Iu., Kovalev R.A., Kopylov A.B., Voronkova Iu.A. Pylevaia obstanovka na rudnike [Dust station on mine]. *Izvestiia Tul'skogo gosudarstvennogo universiteta. Nauki o zemle*, 2018, no. 3, pp. 49-61.

Библиографический список

1. Особенности формирования микроклиматических условий в горных выработках глубоких рудников / В.Н. Карелин, А.В. Кравченко, Л.Ю. Левин, Б.П. Казаков, А.В. Зайцев // Горный журнал. – 2013. – № 6. – С. 65–68.
2. Казаков Б.П., Трушкова Н.А., Зайцев А.В. Применение частичного повторного использования воздуха для снижения количества выпадающей влаги в калийных рудниках // Вестник Пермского национального исследовательского политехнического университета. Геология, нефтегазовое и горное дело. – 2012. – № 3. – С. 129–133.
3. Казаков Б.П., Мальцев С.В., Семин М.А. Способ оптимизации параметров работы нескольких главных вентиляторных установок для проектирования энергоэффективных режимов проветривания рудников сложной топологии // Известия высших учебных заведений. Горный журнал. – 2017. – № 1. – С. 101–108.
4. Поспелов Д.А., Зайцев А.В., Семин М.А. Обоснование максимальной допустимой скорости воздуха в стволах по фактору аэродинамической нагрузки на технологическое оборудование // Горное эхо. – 2020. – № 1. – С. 90–94.
5. Жигула Т.И. Обоснование параметров шахтных многоканатных подъемных установок на основе исследования продольно-поперечных колебаний канатов: дис. … канд. техн. наук. – 1985. – 202 с.
6. Таугер В.М., Волков Е.Б., Леонтьев А.А. Теоретико-механический расчет устойчивости движения сосуда в шахтной скиповой пневмоподъемной установке // Известия Уральского государственного горного университета. – 2018. – № 1 (49).
7. Правила безопасности при ведении горных работ и переработке твердых полезных ископаемых: федеральные нормы и правила в области промышленной безопасности утв. 08.12.2021, № 505. – М., 2021.
8. Brake D.J., Mine Ventilation: A Practitioner's Manual. – Brisbane, Australia, 2013. – 791 c.
9. McPherson M.J. An analysis of the resistance and airflow characteristics of mine shafts // Fourth International Mine Ventilation Congress, 1988. – Brisbane, Queensland. – 8 c.
10. Investigation of Dynamic Load in Superdeep Mine Hoisting Systems Induced by Drum Winding / J. Yao, X. Deng, C. Ma, T. Xu // Shock and Vibration. – 2021. – Т. 2021. – Ст. № 4756813.
11. Единые правила безопасности при разработке рудных, нерудных и россыпных месторождений подземным способом. – М.: Недра, 1972. – 224 с.
12. Белый В.Д. Канатные проводники шахтных подъемных установок. – М.: Углетехиздат. – 1959. – 212 с.
13. Страданченко С.Г., Прокопов А.Ю., Ткачева К.Э. Вероятностный подход к определению временных нагрузок на жесткую армировку вертикальных стволов // Горный информационно-аналитический бюллетень (научно-технический журнал). – 2012. – № 8. – С. 61–68.
14. Chen X. Analysis of the Soviet calculation formula for the clearance between rope-guided conveyance and conveyance // Design of Coal Mine (China). – 1979. – Vol. 26, № 4. – P. 17–23.
15. Chen X. Swing of hoisting conveyance using steel rope guides // Coal Science and Technology (China). – 1985. – Vol. 13, № 2. – P. 23–26.
16. Wu R., Zhu Z., Cao G. Computational Fluid Dynamics Modeling of Rope-Guided Conveyances in Two Typical Kinds of Shaft Layouts // PLoS One. – 2015. – Vol. 17, № 2. – P. 978–987.
17. Simulation of the lateral oscillation of rope-guided conveyance based on fluid-structure interaction / R. Wu, Z. Zhu, G. Chen, G. Cao, W. Li // Journal of Vibroengineering, – 2014. – Vol. 16, № 3. – P. 1555–1563.
18. Vibration Analysis of Winding Hoisting System based on ADAMS/Cable / C. Ma, J. Yao, X. Xiao, X. Di, Y. Jiang // Journal of Physics: Conference Series. – IOP Publishing, 2021. – Vol. 1750, № 1. – Art. № 012033.
19. Wang N., Cao G., Yan L. The Study of Hoisting System for Vertical Shaft Construction Without the Protection of Guided-cable // 8th Symposium on Lift and Escalator Technologies. – 2018. – Vol. 8, № 1. – P. 153–159.
20. Ji-hu B.A.O., Peng Z., Chang-ming Z.H.U. Modeling and control of longitudinal vibration on flexible hoisting systems with time-varying length // Procedia Engineering. – 2011. – Vol. 15. – P. 4521–4526.
21. Повышение энергоэффективности системы вентиляции глубокого рудника за счет изменения аэродинамических параметров скипового ствола / Д.А. Поспелов, А.В. Зайцев, М.А. Семин, С.В. Мальцев, Е.Н. Мизонов // Горный информационно-аналитический бюллетень (научно-технический журнал). – 2021. – № 9. – С. 135–144.
22. Semin M., Levin L. Theoretical study of partially return air flows in vertical mine shafts // Thermal Science and Engineering Progress. – 2021. – Vol. 23. – Art. № 100884.
23. Исследование динамики пылевоздушной смеси при проветривании тупиковой выработки в процессе работы комбайновых комплексов / Л.Ю. Левин, А.Г. Исаевич, М.А. Семин, Р.Р. Газизуллин // Горный журнал. – 2015. – № 1. – С. 72–75.
24. Continuing invariant solutions towards the turbulent flow / E. Parente, M. Farano, J.C. Robinet, P. De Palma, S. Cherubini // Philosophical Transactions of the Royal Society A. – 2022. – Т. 380, № 2226. – Art. № 20210031.
25. Menter F.R. Two-Equation Eddy-Viscosity Turbulence Models for Engineering Applications // AIAA Journal. – 1994. – Vol. 32, № 8. – P. 1598–1605.
26. Adanta D., Fattah I.M.R., Muhammad N.M. Comparison of standard k-epsilon and SST k-omega turbulence model for breastshot waterwheel simulation // Journal of Mechanical Science and Engineering. – 2020. – Vol. 7, № 2. – P. 39–44.
27. Semin M., Golovatyi I., Pugin A. Analysis of Temperature Anomalies during Thermal Monitoring of Frozen Wall Formation // Fluids. – 2021. – Vol. 6. – № 8. – Art. № 297.
28. Ceilometer monitoring of boundary-layer height and its application in evaluating the dilution effect on air pollution / J. Lee, J.W. Hong, K. Lee, J. Hong, E. Velasco, Y.J. Lim, J. Park // Boundary-Layer Meteorology. – 2019. – Vol. 172, № 3. – P. 435–455.
29. Jandaghian Z. Flow and pollutant dispersion model in a 2D urban street canyons using computational fluid dynamics // Computational Engineering and Physical Modeling. – 2018. – Vol. 1, № 1. – P. 83–93.
30. Validation of a fluid–structure interaction model of a heart valve using the dynamic mesh method in fluent / K. Dumont, J.M.A. Stijnen, J. Vierendeels, F.N. Van De Vosse, P.R. Verdonck // Computer methods in biomechanics and biomedical engineering. – 2004. – Vol. 7, № 3. – P. 139–146.
31. A CFD model of frost formation based on dynamic meshes technique via secondary development of ANSYS fluent / Y. You, S. Wang, W. Lv, Y. Chen, U. Gross // International Journal of Heat and Fluid Flow. – 2021. – Т. 89. – Art. № 108807.
32. Mrinal K.R., Siddique M.H., Samad A. A transient 3D CFD model of a progressive cavity pump // Turbo Expo: Power for Land, Sea, and Air. – American Society of Mechanical Engineers, 2016. – Vol. 49873. – Art. № V009T24A009.
33. Mesh smoothing algorithm based on exterior angles split / Y. Hai, S. Cheng, Y. Guo, S. Li // Plos one. – 2020. – Vol. 15, № 5. – Art. № e0232854.
34. Analysis of the effects of dynamic mesh update method on simulating indoor airflow induced by moving objects / H. Zhou, K. Zhong, H. Jia, Y. Kang // Building and Environment. – 2022. – Art. № 108782.
35. Adedeji O.E., Duarte C.A. R. Prediction of thickness loss in a standard 90° elbow using erosion-coupled dynamic mesh // Wear. – 2020. – Vol. 460. – P. 203400.
36. Krige G.J. Guidelines for the design of rope guides // International Conference on Hoisting and Haulage 2005, Perth, Australia. – 2005. – P. 275–283.
37. Русских С.В., Шклярчук Ф.Н. Применение метода Бубнова-Галеркина для расчета нелинейных колебаний математического маятника переменной длины при конечном передвижении из одного состояния покоя в другое // Инженерный журнал: наука и инновации. – 2018. – № 10 (82). – С. 1–15.
38. Суриков И.Ю., Суббота А.Д., Тархов Д.А. Применение новых методов решения дифференциальных уравнений к задаче стабилизации перевернутого маятника // Нейрокомпьютеры и их применение. – 2018. – С. 358–359.
39. Штеттер Х. Анализ методов дискретизации для обыкновенных дифференциальных уравнений. – М.: Мир, 1978. – 461 с.

40. Явная схема расщепления для уравнений Максвелла / И.В. Мингалев [и др.] // Математическое моделирование. – 2018. – Т. 30, № 12. – С. 17–38.
41. Kulshreshtha A., Gupta S.K., Singhal P. FEM/CFD analysis of wings at different angle of attack // Materials Today: Proceedings. – 2020. – Vol. 26. – P. 1638–1643.
42. Computational fluid dynamics simulation of changes in the morphology and airflow dynamics of the upper airways in OSAHS patients after treatment with oral appliances / B. Song, Y. Li, J. Sun, Y. Qi, P. Li, Y. Li, Z. Gu // PloS one. – 2019. – Vol. 14, № 11. – Art. e0219642.
43. Brook R.J., Arnold G.C. Applied regression analysis and experimental design. – CRC Press, 2018.
44. Сравнение точности аппроксимации экспериментальных данных методом наименьших относительных квадратов с методом наименьших квадратов / А.Б. Голованчиков, М.К. Доан, А.В. Петрухин, Н.А. Меренцов // Моделирование, оптимизация и информационные технологии. – 2020. – Т. 8. № 1. – С. 38–39.
45. Левин Л.Ю., Кормщиков Д.С., Семин М.А. Решение задачи оперативного расчета распределения продуктов горения в сети горных выработок // Горный информационно-аналитический бюллетень (научно-технический журнал). – 2013. – № 12. – С. 179–184.
46. Разработка энергосберегающих технологий обеспечения комфортных микроклиматических условий при ведении горных работ / Б.П. Казаков, Л.Ю. Левин, А.В. Шалимов, А.В. Зайцев // Записки Горного института. – 2017. – Т. 223. – С. 116–124.
47. Field measurement and numerical simulation of dust migration in a high-rise building of the mine hoisting system / X. Feng, F. Geng, H. Teng, C. Gui, S. Wu, S. Li, S. Yuan // Environmental Science and Pollution Research. – 2022. – Т. 29, № 25. – С. 38038–38053.
48. Исаевич А.Г., Кормщиков Д.С. Исследование пылевой обстановки в условиях калийного рудника, опыт снижения запыленности атмосферы рабочих мест // Известия Тульского государственного университета. Науки о земле. – 2018. – № 4. – С. 60–74.
49. Пылевая обстановка на руднике / М.Ю. Лискова, Р.А. Ковалев, А.Б. Копылов, Ю.А. Воронкова // Известия Тульского государственного университета. Науки о земле. – 2018. – № 3. – С. 49–61.

Funding. The study was financially supported by the Russian Foundation for Basic Research under the project No. 19-35-90076, and by the Ministry of Science and Higher Education of the Russian Federation under the state assignment No. 075-03-2021-374 dated "29" December 2020 (reg. number R&DKTR 122030100425-6).

Conflict of interest. The authors declare no conflict of interest.

The authors' contribution is equal.